Capability assessment and challenges for quantum technology gravity sensors for near surface terrestrial geophysical surveying

Boddice, Daniel; Metje, Nicole; Tuckwell, George

DOI:
10.1016/j.jappgeo.2017.09.018

Document Version
Publisher's PDF, also known as Version of record

Citation for published version (Harvard):
Boddice, D, Metje, N & Tuckwell, G 2017, 'Capability assessment and challenges for quantum technology gravity sensors for near surface terrestrial geophysical surveying', *Journal of Applied Geophysics*, vol. 146, pp. 149-159. https://doi.org/10.1016/j.jappgeo.2017.09.018

Journal of Applied Geophysics 146 (2017) 149–159

Contents lists available at ScienceDirect

Journal of Applied Geophysics

journal homepage: www.elsevier.com/locate/jappgeo

Capability assessment and challenges for quantum technology gravity sensors for near surface terrestrial geophysical surveying

Daniel Boddice [a,*], Nicole Metje [a], George Tuckwell [b]

[a] School of Engineering, College of Engineering and Physical Sciences, University of Birmingham, Edgbaston, Birmingham B15 2TT, UK
[b] RSK, 18 Frogmore Road, Hemel Hempstead, Hertfordshire HP3 9RT, UK

ARTICLE INFO

Article history:
Received 22 December 2016
Received in revised form 15 August 2017
Accepted 19 September 2017
Available online 28 September 2017

Keywords:
Quantum gravity
Gravity gradiometer
Computer simulation
Civil engineering

ABSTRACT

Geophysical surveying is widely used for the location of subsurface features. Current technology is limited in terms of its resolution (thus size of features it can detect) and penetration depth and a suitable technique is needed to bridge the gap between shallow near surface investigation using techniques such as EM conductivity mapping and GPR commonly used to map the upper 5 m below ground surface, and large features at greater depths detectable using conventional microgravity (>~5 m below ground surface). This will minimise the risks from unknown features buried in and conditions of the ground during civil engineering work. Quantum technology (QT) gravity sensors potentially offer a step-change in technology for locating features which lie outside of the currently detectable range in terms of size and depth, but that potential is currently unknown as field instruments have not been developed. To overcome this, a novel computer simulation was developed for a large range of different targets of interest. The simulation included realistic noise modelling of instrumental, environmental and location sources of noise which limit the accuracy of current microgravity measurements, in order to assess the potential capability of the new QT instruments in realistic situations and determine some of the likely limitations on their implementation.

The results of the simulations for near surface features showed that the new technology is best employed in a gradiometer configuration as opposed to the traditional single sensor gravimeter used by current instruments due to the ability to suppress vibrational environmental noise effects due to common mode rejection between the sensors. A significant improvement in detection capability of 1.5–2 times was observed, putting targets such as mineshafts into the detectability zone which would be a major advantage for subsurface surveying. Thus this research, for the first time, has demonstrated clearly the benefits of QT gravity gradiometer sensors thereby increasing industry's confidence in this new technology.

1. Introduction

Geophysical surveying is widely used for the location of subsurface features and is of key importance for civil engineering (Metje et al., 2011), archaeology (Wynn, 1986), mineral exploration (Watson et al., 1998), environmental studies (Styles, 2012), in the petroleum and hydrocarbon industry (Berger and Anderson, 1981; Finch, 1985) and for unexploded ordinance management (Butler et al., 2002). In civil engineering, it is vital to be able to accurately locate hazards in the near surface prior to construction, as well as assess the condition of the ground in order to reduce the risks of unforeseen or unknown ground conditions when breaking ground or building foundations. This reduces the risks due to excavation as well as saving project costs through reduced Health & Safety impacts and mitigation procedures.

Commonly used geophysical techniques such as ground penetrating radar (GPR), electromagnetic (EM) conductivity, electrical resistivity and seismic methods have been successfully used to locate underground features in the near surface (Table 1). However, these "active" techniques rely on the transmission of generated signals such as EM waves into the ground, which have a limited penetration depth due to the spreading of the signal with distance and attenuative ground conditions. An alternative is to use "passive" technologies such as magnetic or gravity surveying which rely only on being able to measure the potential field generated by the target of interest and to distinguish it from the regional field and signals from other features above or below the ground.

In addition to the signal from the buried target, these instruments also measure noise (defined as spatially and temporally varying signals other than that from the target of interest) which compromises their detection capability and stems from 3 main sources;

1. Instrumental noise stemming from the instrument itself which tends to vary as a function of time. Examples include variation in the

* Corresponding author.
E-mail address: d.boddice@bham.ac.uk (D. Boddice).

https://doi.org/10.1016/j.jappgeo.2017.09.018

orientation of the instrument (e.g. tilt on gravimeters, sensor headings on magnetometers), drift on the sensor and electronic flicker noise from the instrumental electronics.
2. Environmental noise stemming from vibrations and signals from the movements of the planets and seas. These typically vary as a function of both time and spatial location. Examples include tidal signals, changes in atmospheric pressure, vibrational noise from traffic and microseismic noise from ocean waves in microgravity measurements and the presence of changing magnetic fields such as those produced by power cables or moving traffic in magnetic surveying.
3. Location based noise caused by the position of the instrument. These are static as a function of time but vary according to the location of the instrument. Examples include near surface signals from iron debris and buildings in magnetic surveying, and latitude noise, height of the sensor and signals from surrounding buildings and terrain in microgravity surveying.

These geophysical techniques are therefore limited by the resolution of current instruments (which causes quantization errors for small signals) as well as the magnitude of other noise signals and capability to remove them through survey strategy and processing. Details of the potential capability of a wide range of geophysical techniques in terms of horizontal and vertical resolution, and the factors which compromise them in terms of noise are given in Table 1.

In order to gain some idea of how well existing technologies perform in field conditions, experienced operators were consulted and asked for their experience of the performance of the different techniques in terms of the minimum size objects which could be detected in ideal but realistic conditions. Fig. 1 shows the limitations for detection in idealised conditions for four of the most commonly used existing technologies (GPR, Electrical Resistivity, EM conductivity mapping and conventional microgravity) for civil engineering surveys based on spherical features of different diameters buried at a range of depths below the ground surface. These anomalies are taken to have detectable material contrasts which would be typical for expected targets using each technique. For instance, the microgravity and resistivity anomaly is represented by a spherical void whereas the electrical resistivity and EM conductivity anomalies are represented as clay bodies within chalk. In civil engineering ground investigation studies, targets range from pipes and cable ducts with diameters of 0.1–1.2 m in the upper few metres, to larger features such as mineshafts, caves and pingos, which can be several metres in diameter and lie at greater depths of up to 50 m. Whilst it can be seen that these techniques perform reliably for shallow targets and electrical resistivity and conventional microgravity are useful for large targets at depth such as large voids, it is apparent that a large number of smaller objects (<2 m in diameter) at moderate depths (below 10 m) are currently outside the range of detection (see shaded area). It should also be noted that these detection ranges are in optimal conditions and in certain ground conditions, penetration depths could be significantly less. It is therefore apparent that a technique is needed to bridge the gap between the ability to detect large objects at depth and detailed near surface observation.

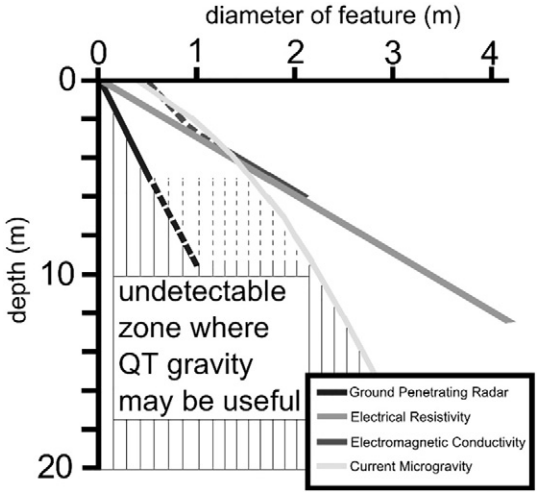

Fig. 1. The detection limits of four different geophysical techniques for spheres with perfect geophysical contrasts of different diameters and depths.

One possible solution to this problem may be to improve the sensitivity of the existing microgravity instruments which, even with long

Table 1
The resolution in the horizontal and vertical directions, depth of penetration and compromising factors for different geophysical techniques.

Instrument	Resolution (H)	Resolution (V)	Depth penetration/detection resolution	Principal compromising factors that would reduce the ability to detect the target[a]
FDEM (e.g. EM31)	±1 m	n/a (upper 5-7 m)	Averages the properties of the upper ~3–7 m of ground	As sensitive to above ground conductivity contrasts (esp. any metal) as to below ground features; Strong local EM fields (e.g. power cables, transmitters, mobile phones)
TDEM (e.g. EM61)	±1 m	n/a (upper 3 m)	Averages the properties of the upper ~3 m of ground.	Strong local EM fields (e.g. power cables, mobile phones)
GPR	1/10 depth	1/10 depth	frequency dependent; e.g. 1GHz–1 m 400 MHz–2 m 100 MHz–6 m	Electrically conductive ground conditions may limit penetration depth; uneven surface may cause air gaps beneath the antenna which will compromise data clarity
Microgravity (e.g. CG5)	1/5 depth	1/3 depth	No depth restriction. 10 μGals (Equivalent to e.g. a 2 m cylinder void at 8 m depth)	Vibration noise; soft/unstable ground; strong free-earth oscillations;, rapidly varying topography; inversion to determine the position and nature of the causative body requires a simple geometry, and little or no other signals in the data. Horizontal resolution dependent upon body geometry and survey design. Vertical resolution often requires additional constraints from other geophysical or investigation data.
Magnetic total field/ gradiometry (surface)	1/5 of depth	1/3 depth	No depth restriction. 0.1 nT e.g. from soil variations associated with archaeological remains	As sensitive to above ground ferrous objects as to below ground ferrous objects; Lateral resolution dependent upon the signal to noise ratio, so will be compromised in areas of high magnetic variability (e.g. igneous geology, areas of high anthropogenic materials). Vertical resolution depends upon the causative body being an isolated feature of known geometry otherwise depth inversions are non-unique.

[a] All techniques seek to detect physical contrasts (density, elastic or electrical) between the target object and the surrounding ground materials. Greater contrasts are more easily detected, as are larger, shallower targets. Deeper, smaller and less contrasting targets are correspondingly more difficult to detect. All anomalies of interest may be masked by the signals/responses generated by other features in the subsurface (or for some technologies also above surface) that may represent equivalent or greater contrasts, and which would therefore mask or compromise the signal detectable from the target feature.

integration times to average out the effects of environmental vibrational noise, are currently limited by the resolution and stability of the mass and spring system and electronic components used which cause the instruments to drift and record low frequency noise. To overcome these limitations, different options for manufacturing instruments to acquire more accurate gravity measurements exist, including superconducting gravimeters (Goodkind, 1999), which offer the highest accuracy but are unsuited to field conditions, and quantum technology (QT) sensors (Freier et al., 2016; Wu, 2009) which offer improved resolution and can be developed as field instruments (Hinton et al., 2017). However, with an expectation of lower intrinsic instrument noise and consequent additional sensitivity to signals generated by buried targets comes an equal increase in the sensitivity to environmental noise effects and signals from other sources such as overlying terrain or deeper regional trends (DiFrancesco et al., 2009). This paper, for the first time, quantifies the practical improvement in detectability for a range of different targets using QT instruments. Furthermore, it proposes the requirements of a new QT sensor for field use and identifies the additional improvements to current commercial survey strategies required to utilise the new QT sensors to their fullest potential and open up the hidden subsurface for safer excavations. It provides the novel forward model essential to interpret the data from the QT sensors under development such that industry can use this novel sensor as soon as it comes to market. Several commercially available QT instruments are now available for use in the laboratory (AOSense, 2017; Muquans, 2017) but these have extensive set up times (up to an hour), require large amounts of power (often from mains sources), have large measurement control units and laptops and are not field ruggedized making them unsuitable for commercial geophysical surveys. The technology also has the potential to be used to measure gravity at two different heights to form a gradiometer but no commercial versions of a QT gravity gradiometer for geophysical land surveying are currently available. However the technology is developing rapidly, and instruments suitable for use in field surveys are likely to be available in the very near future.

2. Data simulation method

In order to assess the capability of the new QT sensors, computer simulations using bespoke MATLAB® scripts were used to model a variety of different features. Industrial stakeholders from a variety of backgrounds were asked for input on their top list of desirable targets which currently are difficult to detect with existing geophysical techniques but present substantial ground risks for civil engineering projects:

- Buried utility services, pipes and tunnels, especially at depths greater than the typical detection range of existing techniques such as GPR (>1.5–2 m).
- Disused mineshafts which typically lie at depths which put them outside the detection capability of existing techniques (>5 m).
- Voids, caves, pingos and solution features.

It should be noted that this list is by no means exhaustive in terms of the potential for QT gravity sensors but shows the priority areas for industry and concentrated the modelling on targets of interest. Each of these targets were defined either as a single or multiple geometric shapes (vertical and horizontal cylinders, spheres and parallelpipeds) which can be modelled using commonly known equations (Kearey et al., 2013; Telford et al., 1990). This was used to generate the gravity signal at a number of discrete points to represent a typical survey grid. The different models along with the fixed and variable parameters are shown in Fig. 2 and the range of variables used for modelling are shown in Table 2.

In order to assess the real world performance, realistic noise was required. Published examples of noise (e.g. Ardhuin et al., 2011; Debeglia and Dupont, 2002; Merriam, 1992; Nowell, 1999) and measurements using several commercial gravimeters (Scintrex CG5) were taken in order to assess the scale and nature of different noise sources which

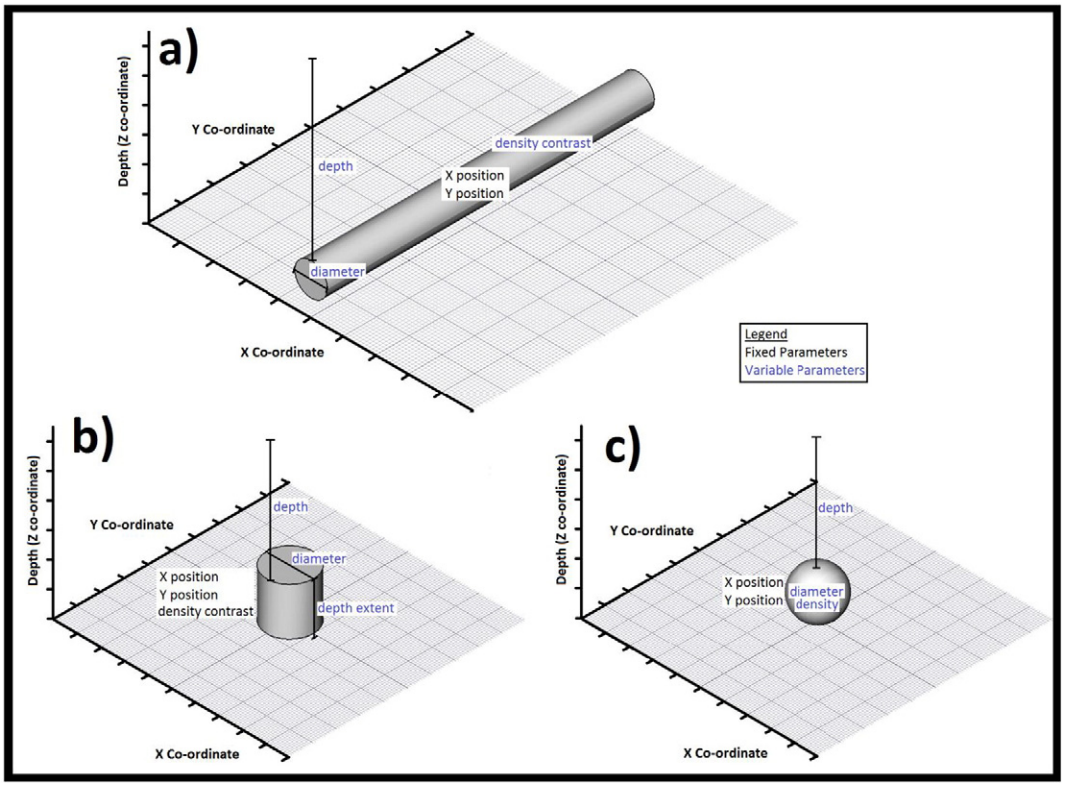

Fig. 2. The different models used for a) pipes and tunnels, b) mineshafts, and c) caves, pingo and voids.

Table 2
The models and ranges of different parameters used for modelling different features. The interval of the variable set is also displayed in brackets.

Feature	Model Shape	Grid size and spacing	Depths	Radii	Length/wavelength	Density
Pipe/tunnel	Horizontal Cylinder	50 × 50 m 2 m spacing	2–10 m (0.5 m)	0.1–4.5 m (0.1 m)	–	gas, fluid
Mineshaft	Vertical Cylinder	50 × 50 m 2 m spacing	5–50 m (5 m)	2–10 m (1 m)	50–1000 m (50 m)	Gas, fluid, rubble
Caves/pingos/solution features	Sphere	75 × 75 m 2 m pacing (depths <15 m) 150 × 150 m 5 m spacing (depths 20–30 m) 250 × 250 m 10 m spacing (depths >30 m)	5–50 m (5 m)	0.5–10 m (0.5 m)	–	Gas, fluid, rubble

are summarised in Table 3. Noise on gravity measurements can be broadly divided into three main types:

1. Instrumental noise which varies as a function of time and the instrument used.
2. Location based noise which is dependent on the location of the measurement point and surrounding features but is non-varying as a function of time
3. Environmental noise which is both dependent on the measurement location and variable as a function of time.

As field capable versions of the new QT sensors do not yet exist, assumptions had to be made with respect to how the different noise sources manifest themselves in the data from the new instrument. Quantification of environmental noise for readings taken using the new instrumentation requires several assumptions to be made, as measurements to study noise have only been taken using existing spring based gravimeter instruments. Firstly, it is anticipated that sources of environmental noise will be transferred to the new instrument by the same mechanisms as the existing instrument and therefore be similar in terms of their nature and magnitude, although the new instrument may be capable of measuring them to a greater degree of accuracy. One additional complication is that additional sources of noise with a magnitude smaller than the maximum resolution of current spring based gravimeters may exist which will only become apparent on measurements with QT instruments. These assumptions are based on published laboratory measurements with QT sensors (Peters et al., 1999; Peters et al., 2001; Snadden et al., 1998). It is also important to note that for the purposes of determining which noise sources will affect the QT gradiometer sensor, an assumption has been made that vibrational noise will affect both the top and bottom sensors of the instrument concurrently and with similar magnitude. This assumption will be true for an ideal gradiometer which meets the following criteria:

1. Individual gravity measurements need to be exactly synchronized in time. Since both atom clouds are measured by a single laser, synchronization is virtually assured allowing for the time taken for the laser beam to reach both atom clouds (i.e. at the speed of light). This gives almost perfect time synchronization
2. Response and noise characteristics of the two individual gravity sensors need to be sufficiently matched. The use of atoms as nature-given, perfectly identical test particles ensures that this criteria is met
3. Measurement axes must be aligned to high precision which is assured in a QT gravity gradiometer system as the same laser is used for the measurement ruler, and the frame must be perfectly rigid which is reasonably achievable using currently available materials and manufacturing techniques.

Since these criteria are met almost perfectly with the proposed QT gradiometer, these noise sources should be substantially reduced in the resulting sensor subtraction (Fig. 3), as evidenced by previous experiments with gravity gradient instruments (e.g. Metzger, 1977; Snadden et al., 1998).

The modelling process for adding noise to the data is summarised in Fig. 4. The simulated data points were each given a synthetic measurement position in terms of latitude, longitude and height, as well as a realistic measurement timestring for each measurement window (3 × 30 s per measurement point at a sampling rate of 6 Hz similar to the current commercial operation of the Scintrex CG5). These were used to generate the different sources of noise following the workflow shown in Fig. 4 and using the methods described in the "method of modelling column" of Table 3 to generate "perfectly" noisy data. However, typically microgravity survey data is corrected to remove or reduce some of the noise sources during data processing using the following typical commercial corrections:

1. Integration of the raw signal to average vibrational noise from wind, waves and nearby anthropogenic activity.
2. Tilt correction using a cosθ function to remove the effects of deviation from vertical gravity
3. Drift removal using linear regression on repeat base station readings to remove the elastic relaxation effects of the instruments quartz spring.
4. Tidal correction using an ephemeris or harmonic model to remove the gravitational signal caused by the sun, moon and other celestial bodies.
5. Latitude correction to account for the non-spherical nature of the earth and subsequent variations in distance from the Earth's gravitational centre of mass using the measurement positions and international gravity formula.
6. Free air correction to account for variations in distance from the Earth's gravitational centre of mass caused by variation in instrument height using the instrument position data and vertical gravity gradient.
7. Bouguer correction to remove the effects of terrain noise caused by the additional mass of underlying ground material and reduce the gravity map to anomalies caused by variations in subsurface density such as those caused by underground voids.

However, the efficacy of many of these corrections is dependent on the accuracy of auxiliary datasets, especially with respect to the spatial location and timing of the measurements which themselves contain errors and result in imperfect subsequent corrections. To represent this, the generated perfect noise was removed imperfectly using corrections based on imperfect auxiliary data to correct survey data to leave a realistic noise source as expected on a typical survey. The following methods were used to apply imperfect corrections:

- Tilts were corrected using the same generated tilt values as used to generate the tilt noise (assuming perfect tilt sensors). However, the corrections were scaled using an average global normal gravity value (980.6×10^9 μGal) rather than the simulated gravity value for each point taking into account the gravity effects of the simulated features which was used to generate the initial noise.

Table 3
Summary of different noise sources on gravity and methods for modelling and correcting them.

	Noise type	Approximate size of error	Correction	Method of modelling
Instrumental noise	Tilt from vertical	0–900μGal (depending on non-linear relationship with tilt).	Minimised by levelling and corrected by internal sensors up to 200 arcseconds tilt in x and y direction with a cos(θ) function and normal gravity	Random tilts between −10 and +10 arcseconds for both the X and the Y axis were generated and used to scale the simulated gravity with a cos(θ) function.
	Linear creep on sensor springs	1–2 mGal per day (instrument dependent)	Linear trend removal from repeat readings over time at base station.	For the existing gravimeter, a random drift constant was generated and used with the timestring to add a linear trend to the data. For QT instruments the drift constant was set to zero.
	Unspecified instrument noise from sensor/electronics	Causes the reading to vary by up to ±2–8 μGal (instrument dependent and longer period than integration time)	None other than by averaging lots of readings per point. Represents the theoretical resolution of the instrument	Normally distributed random numbers were generated and added to the data. Ten times lower instrument noise was used for the QT gravimeter and gradiometer
Environmental noise	Celestial tides	300 μGal a day	Ephemeris and harmonic models, Direct measurement	Generated timestrings, latitudes and longitudes used with a tidal model (Hartmann and Wenzel, 1995) to generate a tidal signal
	Ocean tidal loading	10–20 μGal	Ocean Tide models, Direct measurements.	Generated timestrings, latitudes and longitudes used with an ocean tidal model (Matsumoto et al., 2001) to generate a tidal signal
	Atmospheric pressure	3–7 μGal per day (Pressure dependent; 0.3 μGal per hPa)	Correction to sea level pressure using height and recorded pressure. Complications due to pressure fronts not immediately overhead	Random pressure data is used with the generated timestrings and a pressure formula (Merriam, 1992)
	Seismic and vibrational (anthropogenic, wind noise, ocean wave noise, earthquakes)	Highly dependent on weather and human and seismic activity Wind and Earthquakes give very large disturbances	Windshield (elimination) Averaging over long measurement period, filtering (earthquakes), avoiding trouble spots (reduction)	A random selection of background seismic noise is randomly selected from a library of field surveys and added to the data for each reading
Location noise	Latitude	Depends on latitude (0° = 17 mGal, 90° = 4 mGal) and is non-linear. At mid latitudes c. 0.8 μGal per m.	International gravity formula (Moritz, 1984)	Generated latitude of each measurement point were used with the International gravity formula (Moritz, 1984)
	Height of sensor	308 μGal per m (varies 250–400 μGal per m according to (Lederer, 2009))	Free air correction	Noise is added using the generated height data and a constant of 308 μGal/m
	Terrain effects	Depends on size and proximity of the terrain and the material density	Bouguer Correction (slab or curved plate), DTM model Hammer Correction (poor at localised topology and low sensitivity to small variation)	DTM is used and the gravity signal for each point calculated using vertical prisms above datum height, taking into account both direct and indirect terrain effects.

- Tides were corrected using the latitude and longitude of the central point in the measurement grid and a single measurement time (average of the measurement cycle) rather than the 6 Hz measurement timestring used to create the tidal noise. This generated uncertainty in both the location and time of individual measurements.
- Latitude and free air corrections were generated using imperfect latitude and height data with normally distributed errors with a 95% confidence interval between ±5 mm to represent typical errors on measurement positions on measurements using standard surveying methodologies such as using a total station (e.g. Leica TS15).
- Two types of correction have been trialled for dealing with terrain noise; one based on the Bouguer infinite slab correction (with lower accuracy but still the most common in usage for current commercial gravity surveys (Seigel, 1995)) and another based on a terrain

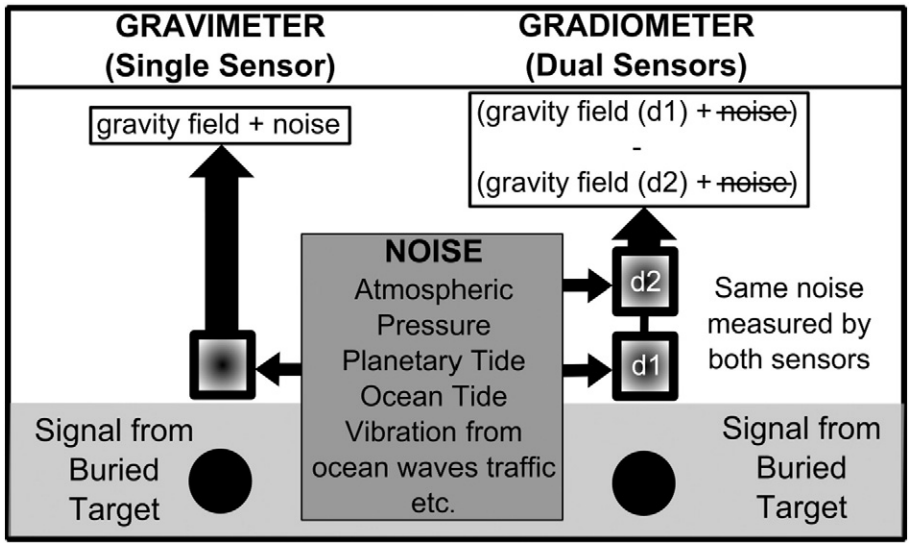

Fig. 3. The noise cancelling effect of the gradiometer configuration in comparison to a conventional gravimeter.

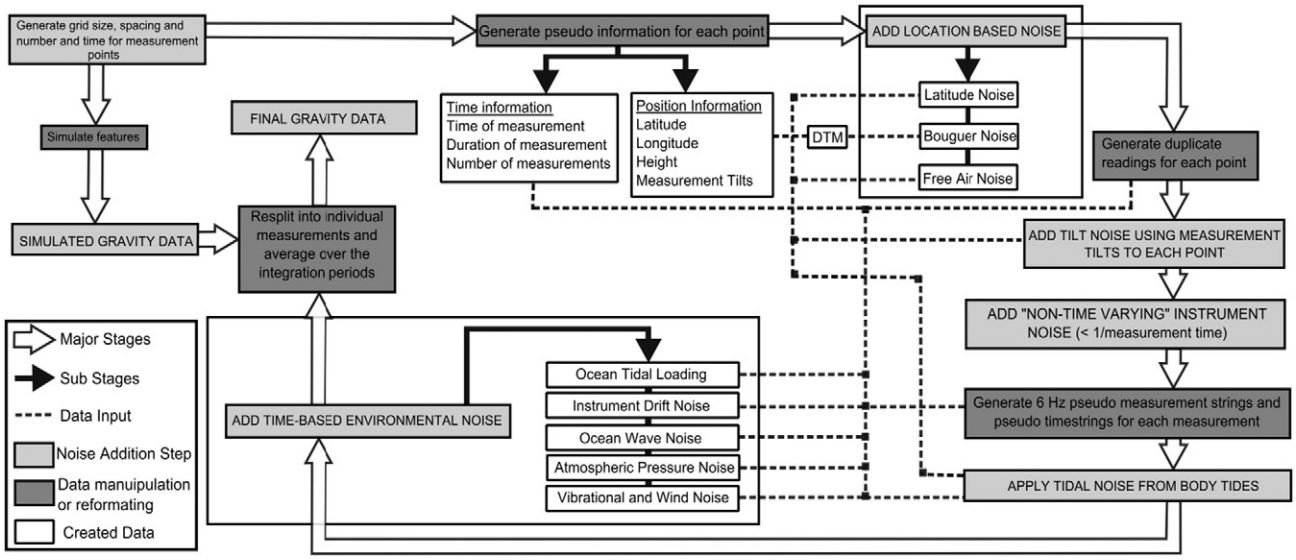

Fig. 4. The data modelling process workflow.

correction calculated from an imperfect digital terrain model (DTM) generated with normally distributed errors with a 95% confidence interval between ±5 mm in all three directions (X, Y and Z). The data were also desampled to a more realistic point density akin to that which could be collected by a surveyor using a total station in a commercially viable timeframe.

Three different sensor configurations were tested; an existing gravimeter based on the Scintrex CG5, a hypothetical QT gravimeter with instrument noise an order of magnitude lower and a QT gradiometer which was created by simulating data at two different heights (1 m apart) and adding identical environmental noise to both simulations, but different location and tidal noise (to account for the difference in height between the two sensors). Instrument noise for the gradiometer was defined as a single value which was added on after the gradient calculation rather than being calculated separately for each sensor. This was intended to represent noise from the measurement system components (laser, vacuum etc.) which will not cancel in the gradient calculation and affect the accuracy of the measurement on each point. Each simulation was run with twenty different noise datasets to represent a range of different topographic and environmental conditions which may be encountered during a survey, and the

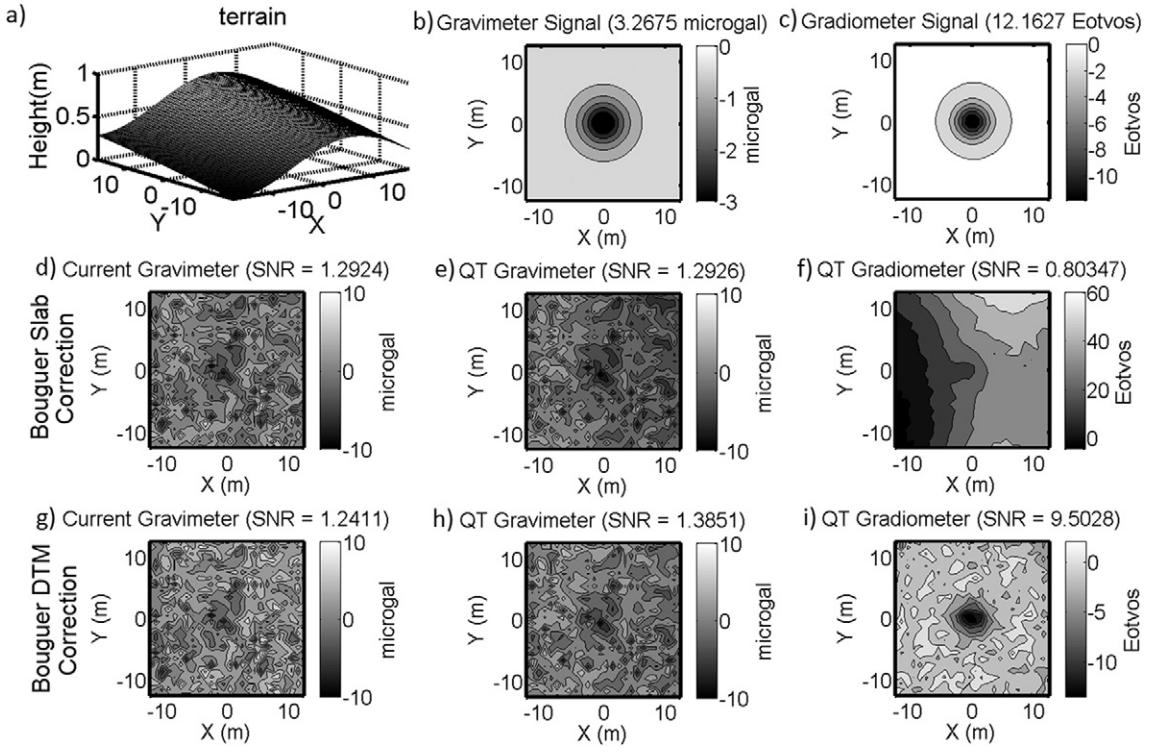

Fig. 5. The effects of different instruments and processing techniques on the visibility of a 1 m radius buried spherical void. a) the terrain model used b) the pure gravity signal with no noise c) the pure gravity gradient signal with no noise d) results from existing gravimeter (Scintrex CG5) and infinite slab correction e) results from QT gravimeter and infinite slab correction f) results from QT gradiometer and infinite slab correction g) results from existing gravimeter (Scintrex CG5) and DTM correction h) results from QT gravimeter and DTM correction i) results from QT gradiometer and DTM correction.

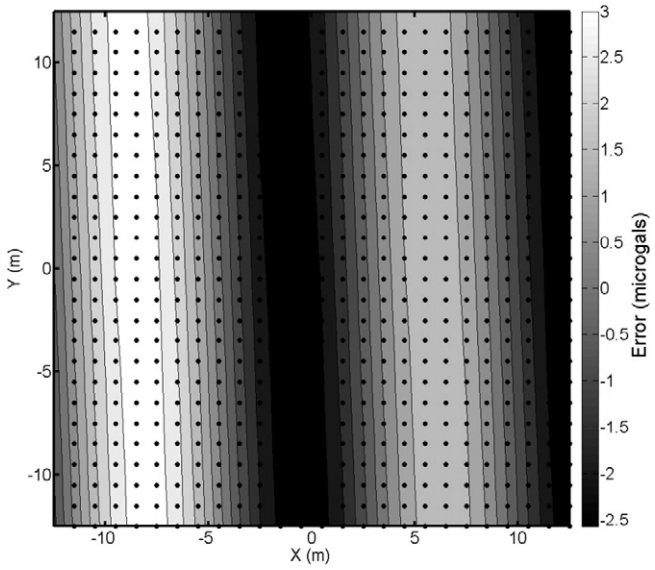

Fig. 6. The errors caused by using the most widely used tidal correction in commercial surveying (Longman, 1959) over a 30 × 30 m grid with a single latitude and longitude input from the centre of the grid and single measurement time per point.

results averaged to produce the detectability maps for the different targets.

3. Results: general observations on the effects of noise on quantum gravity measurements

Fig. 5 shows a typical simulation result for a 1 m spherical void at a depth of 3 m below the ground, with results for all three different instruments (current gravimeter (Figs. 5d, g), QT gravimeter (Figs. 5e, h) and QT gradiometer (Figs. 5f, i) and the effects of slab and DTM corrections. The terrain used for the simulation and the raw signals for the gravimeter and gradiometer are also shown in Figs. 5a-c. Two things are apparent: firstly it is clear that the gradiometer shows far greater potential for the detection of near surface features due to its noise cancelling effects, whereas the QT gravimeter shows only a slight improvement over the current instrument due to the limitations of environmental noise. Secondly, the data demonstrates a clear need to always perform a full DTM correction as opposed to using the Bouguer infinite slab model which is currently in widespread use. This is especially apparent in the difference between the two gradiometer datasets (Fig. 5f and i).

Other corrections also cause significant errors. Fig. 6 shows the errors caused by using the method used by the most widely used tidal correction in commercial surveying based on the Longman model (Longman, 1959) with no ocean tidal loading model along with a single latitude and longitude information for a measurement site (as would be set using the GPS attachment) and a single measurement time for each reading. Over a 30 × 30 m grid, errors of ± 3 μGal can be observed. These errors are unlikely to be currently noticeable due to the instrument noise and practical limitations of current gravimeter repeatability (≈10 μGal) and the common survey practice of using regular (hourly) base station readings to remove linear drifts, which also removes low frequency signals such as these. However, they are likely to have a significant effect on the new more accurate absolute instruments, especially as they have no drift to remove meaning they no longer require regular base stations and drift removal techniques. Future surveys therefore require corrections to be carried out using both more accurate body tide models (e.g. Hartmann and Wenzel, 1995), and models to predict the contribution of ocean tidal loading (e.g. Matsumoto et al., 1995) as well as using more accurate time and location information than in current commercial practice.

These results show that one of the major challenges of applying existing corrections is that due to the increased sensitivity of the new instrument and the inability of the instrument to discriminate between signals from target features and signals from other sources that, in addition to the desired signal, noise sources are also measured with greater accuracy making current corrections insufficient. This highlights the need to collect even higher accuracy supplementary datasets, such as elevation and positional data, and assess the existing corrections for these effects to accurately reduce the data to observe the desired signals.

4. Results: capability maps

Output statistics were used on the large number of simulations to determine the visibility of different features. Peak signals (S) for the gravimeter and gradiometer were defined as the difference between the maximum and minimum values recorded from the simulations of the object without noise. The scale and distribution of the noise was determined by subtracting the original signal from the final noisy data and

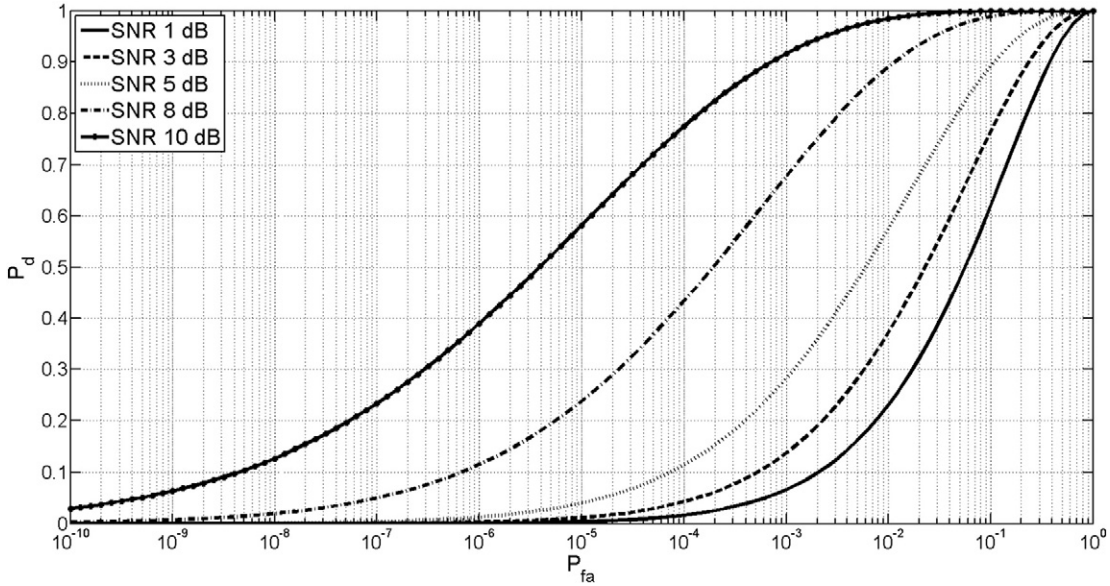

Fig. 7. The relationship between SNR, Probability of false alarm (P_{fa}) and Probability of detection (P_d).

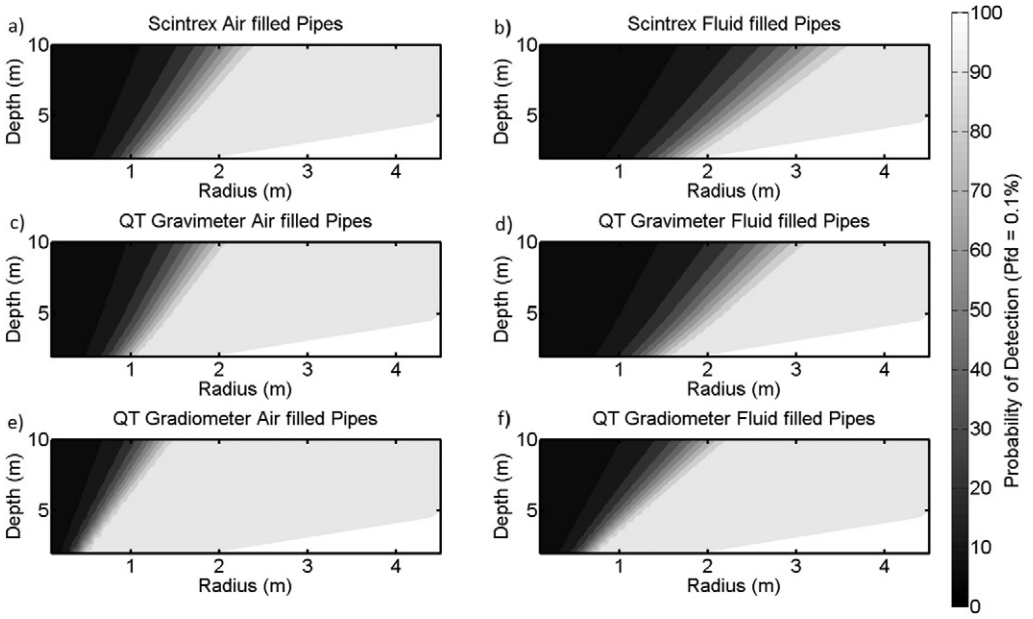

Fig. 8. Detectability maps for pipes and tunnels of different radii and depths for the current gravimeter for air filled (a), fluid filled (b) features, a QT gravimeter for air filled (c), fluid filled (d) features and a QT gradiometer for air fileld (e), fluid filled (f) features.

defined as the standard deviation of these values (SD_N). These two values were used to calculate the signal-to-noise ratio (SNR) using Eq. 1.

$$\mathrm{SNR} = \frac{S}{SD_N} \quad [1]$$

The SNR can be used with the Neyman-Pearson decision rule to determine the probability of detection (P_d) and the probability of a false alarm (P_{fa}) for a given SNR (Poor, 2013) which has the advantage of removing subjectivity and making the results quantitative rather than qualitative. Fig. 7 shows the relationship between P_{fa} and P_d for several different values of SNR. As can be seen the chance of seeing a target in the presence of noise is increased as the P_{fa} increases or the SNR is higher. Testing showed that a value of 0.1% for the P_{fa} gave results in line with visual inspection for the range of models generated in this study, so this value was used to generate the P_d for the detectability maps.

Fig. 8 shows the percentage chance of detecting pipes and tunnels of different radii at different depths below the ground, which were modelled as long (100 m) horizontal cylinders (which are effectively infinitely long for the 50 × 50 m grid used). As would be expected, for all the instruments there is lower chance of detecting fluid filled features due to the lower density contrast, and a greater chance of detecting larger radius pipes. The QT gravimeter (Figs. 8c and d) shows only a

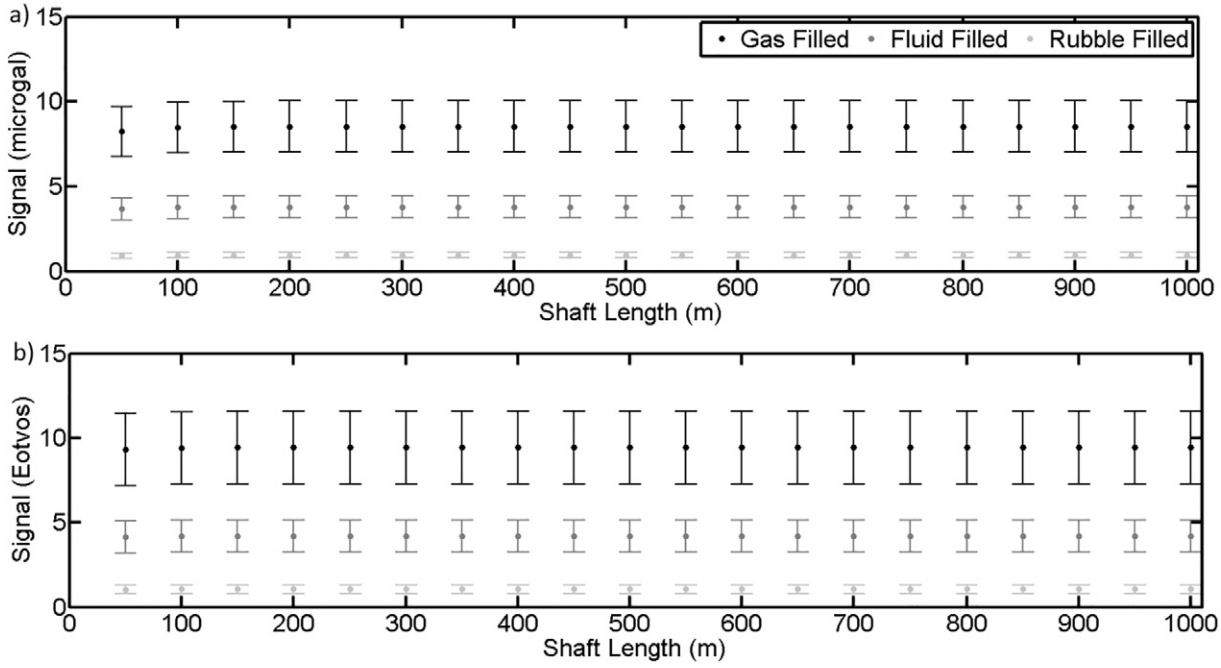

Fig. 9. The effects of different shaft length on the signal from 2 m radius mineshafts at 10 m depth for a) gravimeters and b) gradiometers. Error bars represent 2 SD of the maximum signal strengths from the twenty simulations.

marginal improvement (approximately 1.1–1.2 times better in terms of the minimum size of detectable features) over the existing gravimeter (Figs. 8a and b), whilst the gradiometer configuration (Figs. 8d and e) shows a significant improvement (approximately 1.5–2 times better in terms of the minimum size of detectable features) due to the ability of the instrument to suppress or eliminate sources of vibrational noise.

The detectability of mineshafts was assessed using a vertical cylinder model with variable radii, lengths and depths to the top. The effect of shaft length on the resulting signal is shown in Fig. 9 using a 2 m radius mineshaft with a 10 m depth the top. It can be seen that the shaft length is of very little importance for determining the total signal strength for either the gravimeter or gradiometer configuration. Additional plots of mineshafts (not shown) with other radii and depths showed similar results confirming that the results from different length mineshafts can be averaged to produce the detectability maps as a function of radius and depth which are shown in Fig. 10. Much like the pipes and tunnels, only a slight improvement is offered by the QT gravimeter (Figs. 10d,e and f), with the gradiometer (Figs. 10g,h and i) showing more significant improvements in terms of detection of small, deep objects and those with weaker density contrasts. The level of improvement is of a similar order to those observed in buried pipes (1.5–2 times better than the currently existing sensor in terms of the size and depth of detectable objects).

The detectability maps of spherical caves and pingo features are presented as a function of radius and depth in Fig. 11. As above, the QT gravimeter (Figs. 11d, e and f) showed only a marginal improvement over the results from the existing gravimeter (Figs. 11a, b and c). For near surface targets (<20 m), the gradiometer (Figs. 11g, h and i) performs better, with comparable improvements as for other near surface targets such as pipes and mineshafts. However for targets deeper than this, the configuration performs significantly worse than even the current gravimeter. Neither the QT gravimeter or gradiometer sensors can reliably identify rubble filled caves and pingo features within the tested parameter range due to their low density contrast and these remain a significant risk for ground investigation studies. In addition, fluid filled features were difficult to detect for similar reasons, with only shallow (<10 m) and significantly large (>4 m diameter) features detectable with the QT gradiometer only.

5. Discussion

The detectability maps show the gradiometer configuration performs better in the majority of cases for near surface targets such as pipes, pingos, and mineshafts due the ability of the configuration to suppress or eliminate sources of environmental noise (from ocean waves, anthropogenic activity etc.) through common mode rejection. Much smaller improvements were observed in comparison to existing instruments when using a hypothetical single sensor QT gravimeter configuration despite having significantly lower instrument noise and consequently higher resolution. This was due to effects of the environmental noise which limits the practical resolution based on currently used measuring times for each point. One solution to this problem would be to increase the integration time on each point when using the QT gravimeter, although this has large cost and practicality implications and may be limited by the partially deterministic nature of the vibrational noise. Alternatively, as the QT sensor measures an absolute value of gravity rather than a relative value and therefore readings are theoretically comparable between different instruments, one solution on small scale sites may be to use two instruments; one static instrument to record ambient environmental noise and second rover to collect the points in a 'variometer' configuration similar to similar configurations used in magnetometry surveying (Becker, 2001; Vershovskii et al., 2006). The time varying signal could be subtracted from the measuring points, reducing the measurement time whilst still providing the signal strength of a gravimeter, but the spatial and temporal variation of environmental noise would first need to be well understood. Another possible solution may be to investigate filtering the unwanted signals from the data but this would require good knowledge of the nature of the noises in question and special care to avoid removing useful signals and adding distortions due to under dampening,

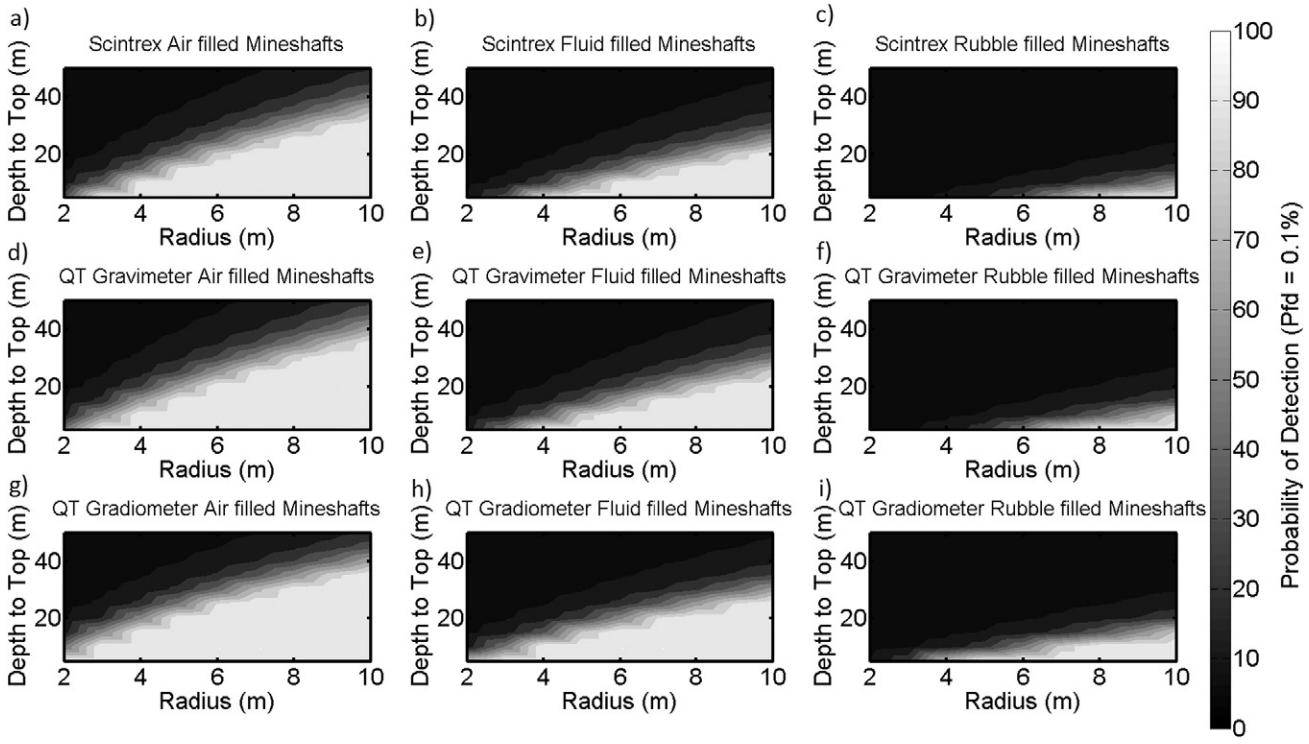

Fig. 10. Detectability maps for mineshafts of different radii and depths for the current gravimeter for air (a), fluid (b) and rubble (c) filled shafts, a QT gravimeter for air (d), fluid (e) and rubble (f) filled shafts and a QT gradiometer for air (g), fluid (h) and rubble (i) filled shafts.

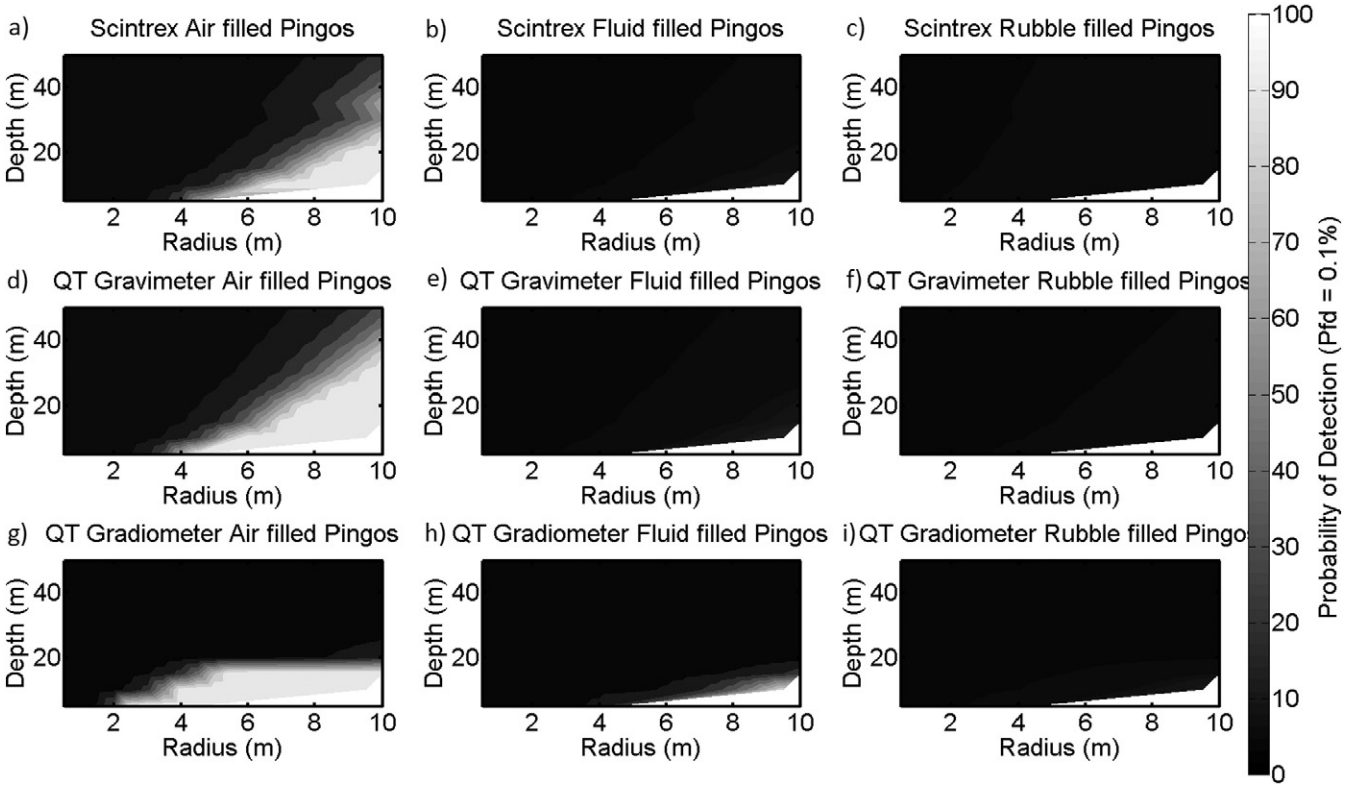

Fig. 11. Detectability maps for caves, solution features and pingos of different radii and depths for the current gravimeter for air (a), fluid (b) and rubble (c) filled features, a QT gravimeter for air (d), fluid (e) and rubble (f) filled features and a QT gradiometer for air (g), fluid (h) and rubble (i) filled features.

and the gradiometer seems like a more commercially viable solution. In contrast, for features such deeper lying pingos, the gradiometer can be seen to perform poorly. This is due to the measurement of the derivative which causes the instrument signal to drop off at a rate of $1/z^3$ (where z is the depth to the feature) as opposed to the $1/z^2$ which characterises the gravity signal. It may be possible to improve the response by either increasing the separation between the top and bottom sensor to increase the signal strength, or by changing the height of the instrument to assist with suppressing near surface noise and further work is needed to investigate this. However, for targets such as these, a traditional single sensor gravimeter configuration may be the preferred option.

It should also be noted that the method for generating the above detectability maps does not account for the spatial distribution of the noise and wavelength in comparison to the signals generated by the buried features. Further improvements may be possible using frequency analysis and spatial filtering techniques in order to suppress signals with different wavelengths to the targets of interest such as those already used in contemporary geophysical practice with a wide range of different techniques (e.g. Linington, 1970; Pawlowski and Hansen, 1990; Zurflueh, 1967).

The simulations have shown though that the significant improvement of a factor of 1.5–2.0 can be expected. Such improvement would represent a huge benefit to the civil engineering and subsurface surveying industry. By providing improved knowledge of buried infrastructure and natural features, excavations can be carried out much safer and cheaper. This has impact for future large-scale infrastructure projects, where a reduction in the risk of unknown ground conditions has significant impacts on project delivery.

6. Conclusions

Numerical simulations of gravity and gravity gradient surveys with realistic noise estimates have been used to predict the capability of gravimeters and gravity gradiometers with characteristics modelled on existing commercial instruments and the hypothetical performance of instruments based on cold atom quantum technology. The results show that with careful corrections, the new sensors an improvement of detectability of a factor of 1.5 to 2.0 is achievable resulting in the ability to detect smaller buried features at depths beyond the limitations of existing geophysical sensors. This allows smaller and deeper targets to be detected, bridging the gap between detailed near surface investigations with existing techniques such as EM conductivity and GPR, and location of larger features at depth with resistivity and conventional gravity surveying. This is a significant finding as it demonstrates the benefits of QT gravity sensors to decrease the risk associated with unforeseen ground conditions and revolutionise the geophysical survey industry.

The study also identified that the gradiometer configuration is superior for measurements of near surface features, whereas the more traditional gravimeter configuration shows more promise for deeper targets such as deeper lying pingos. Thus this research, for the first time, has demonstrated clearly the benefits of QT gravity gradiometer sensors thereby increasing industry's confidence in this new technology. Additional consideration must now also be given to improving the corrections and the collection of auxiliary datasets such as for tides and terrain when conducting a survey. These findings provide a significant contribution for the rapid commercialisation of the new instruments and to make use of their additional sensitivity in geophysical practice.

Acknowledgments

The authors acknowledge the financial support provided by Innovate UK and the Engineering and Physical Sciences Research Council (EPSRC) through the “Study of Industrial Gravity Measurements and Applications (SIGMA) project” EP/M508378/1.

References

Ardhuin, F., Stutzmann, E., Schimmel, M., Mangeney, A., 2011. Ocean wave sources of seismic noise. Journal of Geophysical Research - Oceans 116, C09004.

Becker, H., 2001. Duo- and quadro-sensor configuration for high speed/high resolution magnetic prospecting with caesium magnetometer. In: Becker, H., Fassbinder, J.W.E. (Eds.), Magnetic Prospecting in Archaeological Sites. ICOMOS, Munich, pp. 20–25.
Berger, B.D., Anderson, K.E., 1981. Modern Petroleum: A Basic Primer of the Industry. PennWell Books.
Butler, D., Young, R., Veith, W., 2002. UXO 101: An Introduction to Unexploded Ordinance: Short Course for the Symposium on the Application of Geophysics to Engineering and Environmental Problems (SAGEEP), Las Vegas, NV, February 2002 (Environmental & Engineering Geophysical Society).
Debeglia, N., Dupont, F., 2002. Some critical factors for engineering and environmental microgravity investigations. J. Appl. Geophys. 50, 435–454.
DiFrancesco, D., Grierson, A., Kaputa, D., Meyer, T., 2009. Gravity gradiometer systems – advances and challenges. Geophys. Prospect. 57, 615–623.
Finch, D., 1985. Traces Through Time: The History of Geophysical Exploration for Petroleum in Canada (Canadian Society of Exploration Geophysicists).
Freier, C., Hauth, M., Schkolnik, V., Leykauf, B., Schilling, M., Wziontek, H., Scherneck, H.G., Müller, J., Peters, A., 2016. Mobile quantum gravity sensor with unprecedented stability. J. Phys. Conf. Ser. 723, 012050.
Goodkind, J.M., 1999. The superconducting gravimeter. Rev. Sci. Instrum. 70, 4131–4152.
Hartmann, T., Wenzel, H.-G., 1995. The HW95 tidal potential catalogue. Geophys. Res. Lett. 22, 3553–3556.
Hinton, A., Perea-Ortiz, M., Winch, J., Briggs, J., Freer, S., Moustoukas, D., Powell-Gill, S., Squire, C., Lamb, A., Rammeloo, C., Stray, B., Voulazeris, G., Zhu, L., Kaushik, A., Lien, Y.-H., Niggebaum, A., Rodgers, A., Stabrawa, A., Boddice, D., Plant, S.R., Tuckwell, G.W., Bongs, K., Metje, N., Holynski, M., 2017. A portable magneto-optical trap with prospects for atom interferometry in civil engineering. Philosophical Transactions of the Royal Society A: Mathematical, Physical and Engineering Sciences. 375.
AOSense, 2017. http://aosense.com/solutions/gravimeter/.
Kearey, P., Brooks, M., Hill, I., 2013. An Introduction to Geophysical Exploration. Blackwell, Oxford.
Lederer, M., 2009. Accuracy of the relative gravity measurement. Acta Geodyn Geomater 6, 383–390.
Linington, R.E., 1970. A first use of linear filtering techniques on archaeological prospecting results. Prospezioni Archeologiche 5, 43–54.
Longman, I.M., 1959. Formulas for computing the tidal accelerations due to the moon and the sun. J. Geophys. Res. 64, 2351–2355.
Matsumoto, K., Ooe, M., Sato, T., Segawa, J., 1995. Ocean tide model obtained from TOPEX/POSEIDON altimetry data. J. Geophys. Res. 100 (C12), 319–330.
Matsumoto, K., Sato, T., Takanezawa, T., Ooe, M., 2001. GOTIC2: a program for computation of oceanic tidal loading effect. J. Geol. Soc. Jpn. 47, 243–248.
Merriam, J.B., 1992. Atmospheric pressure and gravity. Geophys. J. Int. 109, 488–500.
Metje, N., Chapman, D.N., Rogers, C.D.F., Bongs, K., 2011. Seeing through the ground: the potential of gravity gradient as a complementary technology. Advances in Civil Engineering Vol. 2011, Article ID 903758.
Metzger, E., 1977. Recent Gravity Gradiometer Developments. Guidance and Control Conference, American Institute of Aeronautics and Astronautics.
Moritz, H., 1984. Geodetic reference system 1980. Bull. Géod. 58, 388–398.
Muquans, 2017. Muquans Absolute Quantum Gravimeter Product Page.
Nowell, D.A.G., 1999. Gravity terrain corrections — an overview. J. Appl. Geophys. 42, 117–134.
Pawlowski, R., Hansen, R., 1990. Gravity anomaly separation by Wiener filtering. Geophysics 55, 539–548.
Peters, A., Chung, K.Y., Chu, S., 1999. Measurement of gravitational acceleration by dropping atoms. Nature 400, 849–852.
Peters, A., Chung, K.Y., Chu, S., 2001. High-precision gravity measurements using atom interferometry. Metrologia 38, 25.
Poor, H.V., 2013. An Introduction to Signal Detection and Estimation (Springer New York).
Seigel, H.O., 1995. A Guide to High Precision Land Gravimeter Surveys. Scintrex Ltd., Concord, Ontario.
Snadden, M.J., McGuirk, J.M., Bouyer, P., Haritos, K.G., Kasevich, M.A., 1998. Measurement of the earth's gravity gradient with an atom interferometer-based gravity gradiometer. Phys. Rev. Lett. 81, 971–974.
Styles, P., 2012. Environmental Geophysics: Everything You Ever Wanted (needed!) to Know But Were Afraid to Ask! (European Association of Geoscientists & Engineers).
Telford, W.M., Geldart, L.P., Sheriff, R.E., 1990. Applied Geophysics. Cambridge University Press.
Vershovskii, A.K., Balabas, M.V., Ivanov, A.É., Kulyasov, V.N., Pazgalev, A.S., Aleksandrov, E.B., 2006. Fast three-component magnetometer-variometer based on a cesium sensor. Tech. Phys. 51, 112–117.
Watson, K., Fitterman, D., Saltus, R.W., McCafferty, A., Swayze, G., Church, S., Smith, K., Goldhaber, M., Robson, S., McMahon, P., 1998. Application of geophysical techniques to minerals related environmental problems. U.S. Geological Survey Open-File Report. U.S. Government Printing Office, Washington, D.C.
Wu, X., 2009. Gravity Gradient Survey With a Mobile Atom Inferometer. Stanford University.
Wynn, J.C., 1986. A review of geophysical methods used in archaeology. Geoarchaeology 1, 245–257.
Zurflueh, E., 1967. Applications of two-dimensional linear wavelength filtering. Geophysics 32, 1015–1035.